International Journal of Industrial Chemistry (2018) 9:27–38
https://doi.org/10.1007/s40090-018-0141-8

RESEARCH

Catalytic oxidation of SO_2 by novel Mn/copper slag nanocatalyst and optimization by Box-Behnken design

Fattah Rabiee[1] · **Kazem Mahanpoor**[1]

Received: 18 November 2016 / Accepted: 12 March 2018 / Published online: 5 April 2018

Abstract
In this research, the oxidation of sulfur dioxide (SO_2) gases is investigated by Mn/copper slag nanocatalyst (Mn/CS) as a novel catalyst at low temperatures. The removal of SO_2 gas from industrial exhaust is important to reduce environmental pollution. The SO_2 gas in aqueous solution was oxidized and converted to sulfuric acid as an energy source by Mn/CS in the semi-batch reactor (SBR). The characterization of the catalyst was studied using X-ray diffraction (XRD), energy-dispersive X-ray spectroscopy (EDX), field emission scanning electron microscopy (FESEM), and Fourier transform infrared spectroscopy (FTIR), simultaneous thermal analysis (thermogravimetry/differential thermal analysis) STA (TG/DTA) techniques, X-ray fluorescence microscopy (XRF) and BET surface area. A Box-Behnken design (BBD) was used for the optimization of influencing factors such as the amount of nanocatalyst, the temperature and the reaction time in the oxidation of SO_2. The graphical counter plots and response surface were used to determine the optimum conditions. The results showed that the nanocatalyst had the most significant effect on SO_2 oxidation compared with the other two variables. Temperature = 283 K, Mn/CS amount = 6 g/L and Time = 60 min were determined as maximum efficiency for oxidation of SO_2.

Keywords SO_2 oxidation · Mn/copper slag nanocatalyst · Box-Behnken design · Optimization

Introduction

Sulfur dioxide (SO_2) and other gases emitted from specific resources are major pollutants of air. These gases create problems for humans, such as acid rain. There are many processes to reduce sulfur dioxide and other pollutants from the air. Among these methods, the process of removing SO_2 at low temperatures is important. These methods require less energy and equipment [1].

Removal of sulfur dioxide from gas emissions using absorption is a common method to reduce air pollution and environmental risks [2]. Activated carbon and zeolite constitute an exciting group of catalysts, which have been presented recently as potential catalysts for the oxidation of SO_2 to sulfuric acid [3, 4]. Some transition metal ions such as Mn or Cu have been reported for the catalytic oxidation of SO_2 [5].

Mn^{2+} has shown to be a very active catalyst for oxidation of SO_2 in aqueous solution [6]. Copper slag has high mechanical strength and high resistance to temperature changes. It seems to be a suitable material to support Mn ions. In the metallurgical industry, copper slag is produced as a byproduct of the smelting process [7]. Mechanical stability and acidic solution resistance, suitable surface for supporting catalyst on it, non-coagulation and geometric shape and high temperature resistance are the most important properties of copper slag [8]. Optimizing processes reduce costs and increase productivity. Recently, response surface method (RSM) is a mathematical and statistical technique used for modeling and optimization of various processes such as removal of organic and many dyes from different wastewater by different process [9–12]. The Box-Behnken design (BBD) in RSM is an important design, implement used for optimization of processes. BBD prepares comprehensive results and detailed information even for a smaller number of experiments and positive influences of operating parameters on all responses [13]. The main goal of this study is to optimize the efficiency of SO_2 catalytic oxidation in

✉ Kazem Mahanpoor
k-mahanpoor@iau-arak.ac.ir

Fattah Rabiee
f-rabiee@iau-arak.ac.ir

[1] Department of Chemistry, Arak Branch, Islamic Azad University, P.O. Box 38135-567, Arak, Iran

aqueous solution. In current research, a novel Mn/copper slags nanocatalyst prepared by impregnation method and characterized by XRD, FESEM, EDX and FTIR analysis. The conductometry method is a powerful tool for monitoring SO_2 oxidation and used for determination of catalyst performance. A Box-Behnken design was selected to study the effects of operational parameter such as temperature, reaction time, and amount of nanocatalyst on the efficiency of the SO_2 oxidation process.

Experimental procedure

Material and apparatuses

Copper slag samples were purchased from Mesbareh Company, Kerman, Iran. The copper-slag-based standard is measured using a glass slide. Hardness of copper slag was much more than silica. Density of copper slag was (3.5 g/cm^3). All of the standard gases included N_2, O_2, SO_2 with purity > 99.9% and were purchased from Gas Company, Iran. Other materials were provided by Merck Company. The characterizations of copper slag and Mn/CS were identified using XRD (STOE STADI MP model Germany), FTIR spectrophotometer (PerkinElmer, a spectrum American with the KBr pellet technique), FESEM, EDX (MIRA3-XMU, USA) and XRF (Model: JSX 3201Z). The differential thermal analysis/thermogravimetric analysis (DTA/TG) experiments were carried out in a Netzsch STA 409 C simultaneous thermal analysis (STA). The samples were kept at 100 °C for 30 min, the heating rates were 25 (°C/min) to a final temperature of 1200 °C. BET surface area of materials was determined by N_2 adsorption–desorption method at 77 K, measured using a BELSORP-mini II instrument. The samples were degassed under vacuum at 473 K for 12 h before the BET measurement. The measurements of pH value were performed by a pH meter (Metrohm model 827, Switzerland with an electrode of glass). The pH meter was calibrated before use, with standard buffers (pH 4.0, pH 7.0 and pH 9.0). Input and output gas of the process was identified by a flue gas analyzer (KIGAZ 300, Kimo Company, France). The experimental setup is shown in Fig. 1. The pH and conductivity measurement (Metrohm Model 712) was used for checking the progress of oxidation reaction. The reactor temperature was controlled by external jackets and thermo-bath (RW-0525G).

Preparation of nanocatalyst and oxidation procedure

For activation of copper slag, 100 g of copper slag was added to 500 ml sulfuric acid solution (0.1 M). The sulfuric acid solution was heated to 60° C. The copper slag remained in the hot sulfuric acid solution to 5 h. Copper slags were isolated from acid solution. Copper slags were washed with distilled water several times and finally washed with ethanol. Then samples were dried at 110 °C for 10 h in the oven.

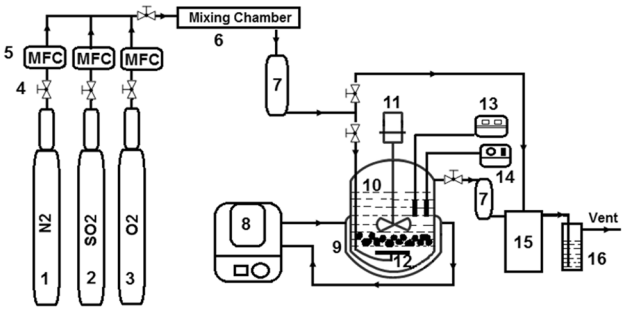

Fig. 1 Schematic diagram of experimental system: (*1–3*) N_2, O_2, SO_2 gas cylinder, (*4*) valve; (*5*) mass flow controller (MFC); (*6*) mixing chamber; (*7*) dryer; (*8*) thermo-bath; (*9*) thermal-jacket; (*10*) semi-batch reactor; (*11*) mixer; (*12*) gas distributor; (*13*) conductometer; (*14*) pH meter; (*15*) gas analyzer; (*16*) tail gas absorber

The Mn/CS was prepared by impregnation method; this method has been used in fluidized, suspended and magnetic ion exchange forms [14, 15]. On this basis, the copper slags were placed in aqueous solution including Mn $(NO_3)_2$ (50%W/V) for 24 h at 60 °C and stirring mixture. After separating the copper slag from this solution, samples were dried at 100 °C for 5 h [16]. Active copper slag and Mn/CS were analyzed by XRD, FTIR, FESEM, TG/DTA, XRF and EDX. In the oxidation process, a gas flow (contains 3000 ppm of SO_2 and 5% of O_2 in N_2) was blown into 250 ml of deionized water in the semi-batch reactor (SBR) until getting a constant conductivity value of 570 µS/cm (corresponds to a HSO_3^- concentration of 1.65×10^{-3} M) [5]. The changes in the electrical conductivity of the solution were measured by the conductivity meter cell in the reactor. The gas (in the constant pressure) was bubbled with the gas diffuser to surface of catalyst particles. The schematic diagram of the experimental setup for catalytic oxidation of SO_2 gas was illustrated with Fig. 1.

Results and discussion

Nanocatalysts' characterization

XRD investigation

Analysis of XRD can be utilized to measure peak broadening with crystallite size and lattice strain due to dislocation [17], thus XRD analysis was performed through Cu $k\alpha$ radiation. The data that shows intensity is plotted in a graph based on 2θ on a range of 10°–90°. Figure 2, shows the X-ray diffraction (XRD) pattern of Mn/CS prepared

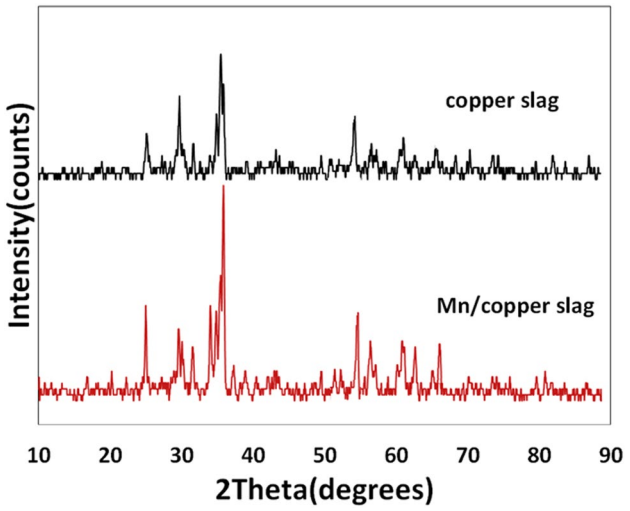

Fig. 2 XRD patterns, copper slag and Mn/copper slag nanocatalyst

by the impregnation method. The results showed that Mn/CS is well matched with copper slag structure. This indicates that the structure of copper slag is unaltered during the impregnation process. The average crystallite size of the Mn/CS was calculated applying the Debye–Scherer equation [18, 19]:

$$d = \frac{k\lambda}{\beta \cos\theta} \quad (1)$$

where k equals to 0.9 and β is the perfect width at half- maximum (FWHM) of the peak, λ is the wavelength of X-ray used 1.54056 A and θ is the Brage angle. The results showed that the Mn is established on the CS with an average diameter of about 68.43 nm.

Field emission scanning electron microscopy (FESEM) investigation

As can be seen from Fig. 3, the prepared nanocatalyst (Mn/CS) is depicted by the field emission scanning electron microscopy (FESEM). The surface morphology and size of samples were identified with FESEM images (before and after the stabilization of manganese). As seen in these images, particle size of the catalyst surface is not equal and also their structure is crystalline. For these reasons, porosity in the Mn/CS was increased.

Energy-dispersive X-ray spectroscopy investigation

The result of the energy-dispersive X-ray spectroscopy (EDX) analyses (Fig. 4, Table 1) shows that the amount of manganese fixed on copper slag is equal to 11.37 wt%. Thus, the EDX confirmed the coating of manganese on the copper slag.

FTIR spectroscopy investigation

The FTIR spectra of the studied samples are presented in Fig. 5. The copper slag FTIR spectrum in the wave number ranges 400–4000 cm^{-1} with a resolution of 4 cm^{-1} by accumulating 32 scans was studied. The wave number accuracy is 0.01 cm^{-1} and the sampling resolution was 0.09 cm^{-1}, therefore by this method, were identified the functional groups. A peak at 3950 cm^{-1} exhibited the hydrate minerals such as $Mn(OH)_2$ and the peak around 3530 cm^{-1} shows the S–O stretch such as the $MnSO_4$. The peak of around 1592 cm^{-1} relates to the C-O asymmetric stretching, whereas a peak at 1408 cm^{-1} may be due to the bonding in the carbonate ions, indicating the presence of some carbonated mineral, possibly due to the adsorption of CO_2 from the atmosphere. The obtained FTIR spectra of copper slag

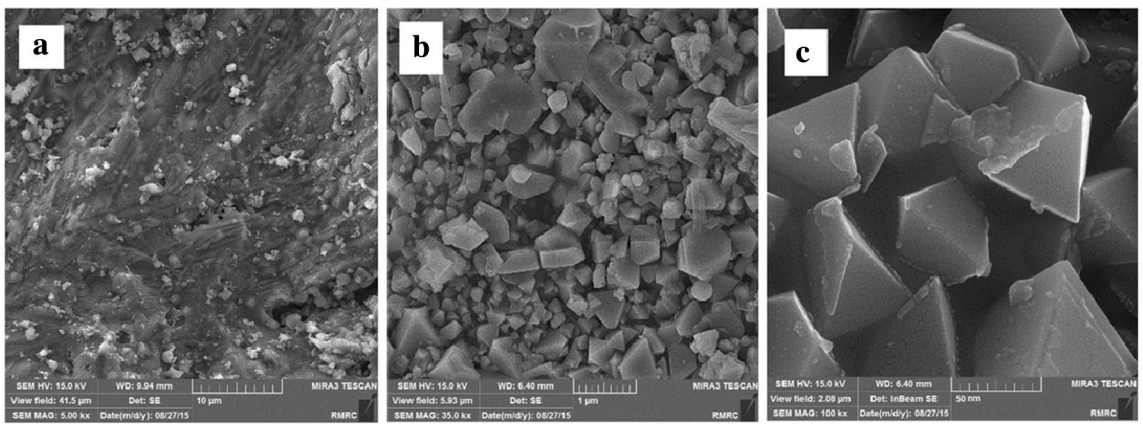

Fig. 3 FESEM images **a** copper slag and **b**, **c** Mn/copper slag

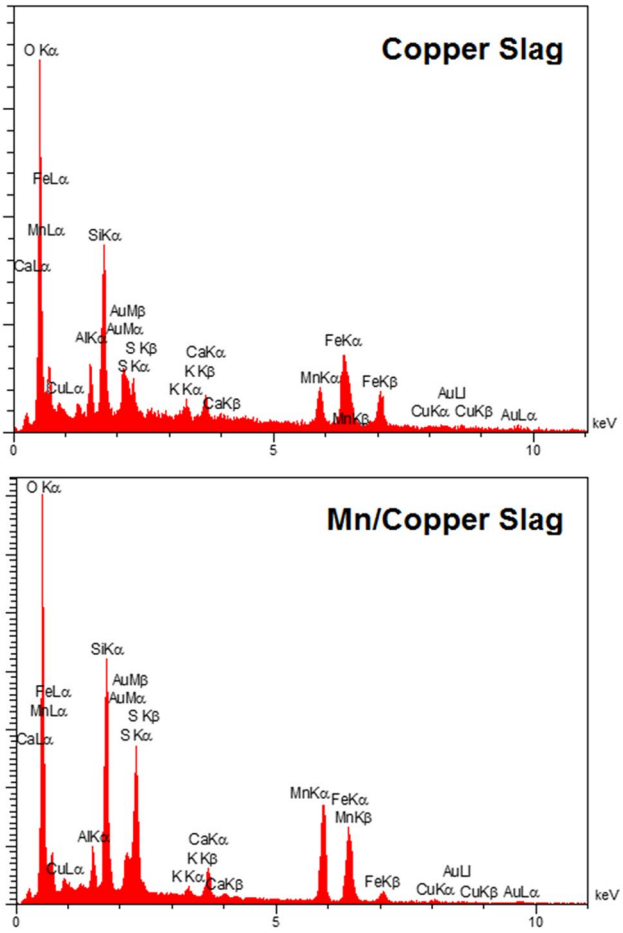

Fig. 4 EDX analyses patterns of copper slag and Mn/copper slag

samples corresponded almost entirely to the spectrum of the Tephroite phase (a-Mn_2SiO_4). This made possible the use of FTIR to determine the composition of tephroite through the established dependency on spectrum bands position on tephroite composition. Adsorption wave number in the spectrum determines the chemical structure of the copper slag. The broad absorption bands of the range of 3100–3600 cm^{-1} are corresponding to the O–H stretching vibration of water that samples were adsorbed. As shown in Fig. 5 the tephroite structure was appeared in 3487–3576 cm^{-1} IR bond [20]. This band represents the main stretching vibrations of different OH^- groups present in Mn–OH–Al, Al–OH–Al, and Fe–OH–Al units in the octahedral layer therefore sulfur dioxide is an acid gas, active sites accountable for adsorption should have a basic structure [20]. After nanocatalyst preparation, the wavenumber is shifted from 610 to 640 cm^{-1} and of sharp bands at 636 and 1609 cm^{-1}, corresponding to Si–O stretching modes of bulk sulphates, mainly $MnSO_4$, in agreement with data from XRD Fig. 2. The peaks of 1150 and 1610 cm^{-1} are the Si–O and Al–O stretching, the peak of 520 cm^{-1} is the C–O bending and the bands of 510 and 490 cm^{-1} are due to Al–O–Si and Si–O–Si bending vibrations, respectively. The FTIR results have proven that Mn as well as placed on the surface of the copper slag.

Simultaneous thermal analysis (STA) results

Figure 6 shows the STA results of a Mn/CS sample. The TG curve reveals the occurrence of a marked weight gain in the 375.18–997.84 °C range, following by a weight loss from 997.84 to 1040.13 °C and then slowly decreases weight region of 1040–1200 °C. The exothermic peaks at 515.47 and 765.12 °C in DTA trace can be related to the magnetite → maghemite and maghemite → hematite transformations, respectively [21]. The endothermic dip at 1040 °C probably can be associated with the slag melting.

XRF characterization

In order to determine the catalyst chemical composition XRF was carried out (Table 2). Based on the results, the percentage of manganese in the Mn/CS sample is greater than that of Cs. These values confirm the EDX results.

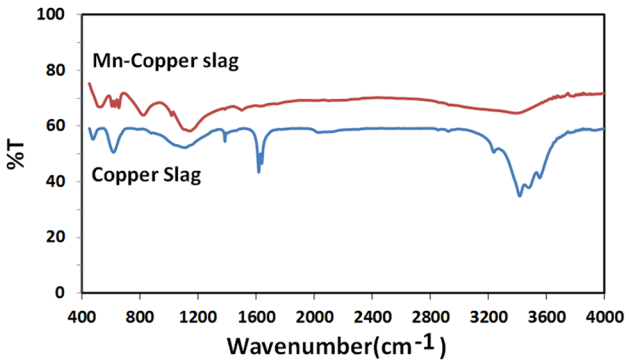

Fig. 5 FTIR spectra of the studied materials: copper slag and Mn/copper slag

Table 1 Elemental analyses of copper slag and Mn/copper slag

Element	Percent	O	Al	Si	S	K	Ca	Mn	Fe	Cu
Copper slag	Wt (%)	38.72	1.45	9.63	6.42	0.51	1.94	5.76	18.16	3.09
	Atomic (%)	61.34	1.36	8.67	5.07	0.33	1.22	4.17	8.23	1.24
Mn/copper slag	Wt (%)	41.76	1.63	8.03	7.22	0.65	2.14	11.37	16.35	1.12
	Atomic (%)	66.16	1.53	7.23	5.7	0.42	1.35	8.23	7.41	0.45

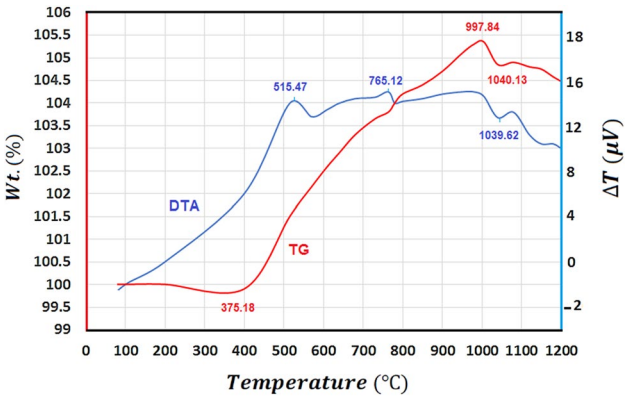

Fig. 6 STA (TG/DTA) traces of Mn/copper slag

Table 2 XRF analyses of copper slag and Mn/copper slag

Composition	Percent (w/w%)	
	Copper slag (CS)	Mn/copper slag (Mn/CS)
SiO_2	25.28	20.93
Al_2O_3	3.47	3.86
CaO	3.18	3.52
Fe_2O_3	32.16	28.43
MnO	8.92	19.13
SO_3	19.82	20.43
K_2O	0.73	0.68
CuO	4.93	1.65
Loss on ignition (LOI)	1.51	1.37

Figure 7 shows the adsorption–desorption isotherms and BET surface area for the Copper slag, and Mn/CS. The BET surfaces area of Copper slag, and Mn/CS were determined 152.46 and 268.37 (m^2/g) respectively. It seems that supporting of nano particle Mn on the CS has been increasing the BET surface area of the catalyst.

Catalytic activity

The schematic diagram of the reactor system was shown in Fig. 1. The catalytic reaction was carried out in a glass reactor (glass thickness 80 mm). The sulfur dioxide gases in the presence of a catalyst and water-soluble oxygen performs the following reactions [22]:

$$SO_{2(g)} + H_2O \rightarrow HSO^-_{3(aq)} + H^+ \quad (2)$$

$$HSO^-_{3(aq)} + \frac{1}{2}O_2 \xrightarrow{\text{catalyst}} SO^{2-}_4 + H^+ \quad (3)$$

$$SO_{2(g)} + \frac{1}{2}O_2 + H_2O \xrightarrow{\text{catalyst}} SO^{2-}_4 + 2H^+ \quad (4)$$

As shown in Eqs. (2–4), the products of the oxidation of SO_2 are SO^{2-}_4 and H^+. Thus, the oxidation of the SO_2 can be directly related to the change in solution conductivity and pH. Effect of catalyst (Mn/CS) amounts to conductivity and pH of solution show in Figs. 8 and 9.

With the advancement of the reaction, the concentration of hydrogen and sulfate ions increases and the electrical conductivity of the solution increases and pH of solution decrease. If the catalyst is not present, the electrical conductivity of the solution and pH will remain constant. Therefore, the reaction is not carried out without the presence of a catalyst.

The results of these experiments used for Box-Behnken experimental design. The present study, based on SO_2 gas, was carried out at considerably lowered temperatures of SO_2.

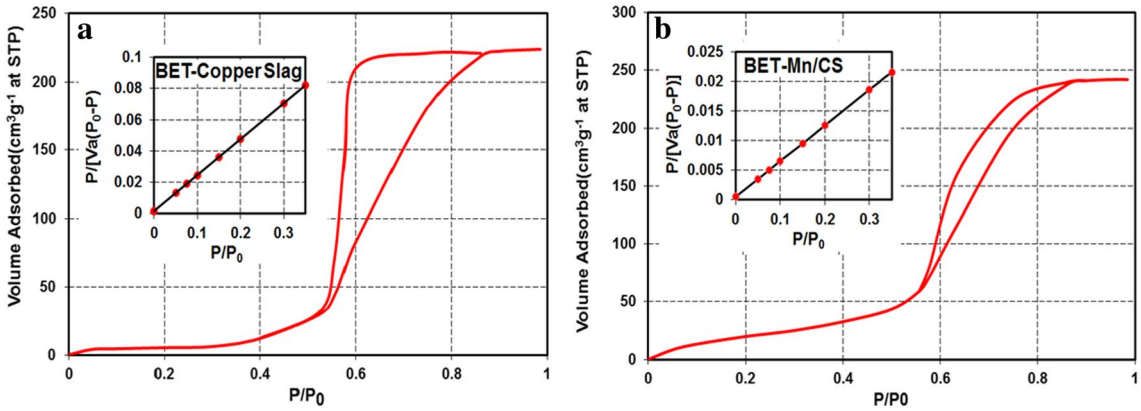

Fig. 7 Adsorption–desorption isotherms and BET surface area for the copper slag (**a**) and Mn/CS (**b**)

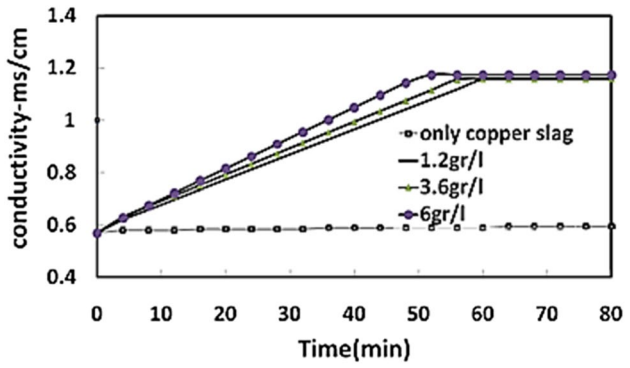

Fig. 8 Conductivity variation for different amounts of (Mn/CS)

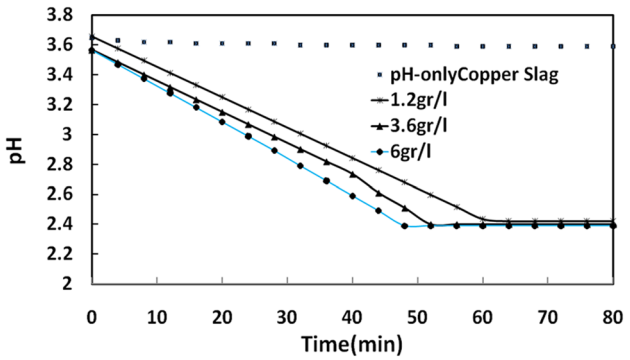

Fig. 9 Effect of amounts of Mn/CS on solution pH

The oxidation efficiency of nanocatalyst for SO_2 is calculated using the following Eq. (5):

$$\eta = \frac{|Ec_{in} - Ec_{fi}|}{Ec_{in}} \times 100 \quad (5)$$

Where SO_2 oxidation efficiency η (%) is, Ec_{in} is the initial conductivity of SO_2 aqueous solution (0.570 mS/cm), Ec_{fi} is the final conductivity of aqueous solution.

The proposed mechanism

Iron, copper and manganese are present in the form of oxides or hydroxides at the copper slag surface metal oxides play an important role in the industrially employed heterogeneously catalyzed autoxidation of sulfur(IV) oxides, for example the production of sulfuric acid with the help of vanadium pentoxide as catalyst. These activities probably depend on the nature of the metal oxide or hydroxide. In general, metal oxides exhibit different catalytic activity, which is probably related to the different bond strengths of oxygen to the metal surface. The catalytic activity of a metal oxide increases with decreasing energy of the metal–oxygen bond. For the heterogeneous oxidation of sulfur(IV) oxides, it is assumed that both oxygen and sulfur(IV) are adsorbed on the surface of the metal oxide [4].

In reaction with oxygen Mn^{2+}/CS is converted to Mn^{3+}/CS [4, 22]:

$$Mn^{2+}/CS + O_2 \rightarrow Mn^{3+}/CS + O_2^- \quad (6)$$

Sulfur dioxide gases dissolved in water and then carry out the following reactions:

$$SO_2 \cdot H_2O \rightleftarrows H^+ + HSO_3^- \quad (7)$$

$$HSO_3^- \rightleftarrows H^+ + SO_3^{2-} \quad (8)$$

Mn^{2+}/CS and Mn^{3+}/CS performs the following reactions:

$$Mn^{2+}/CS + HSO_3^- \rightleftarrows Mn^{2+}/CS + SO_3^{2-} + H^+ \quad (9)$$

$$Mn^{3+}/CS + HSO_3^- \rightleftarrows Mn^{2+}/CS + SO_3^- + H^+ \quad (10)$$

$$Mn^{3+}/CS + SO_3^{2-} \rightleftarrows Mn^{2+}/CS + SO_3^- \quad (11)$$

The SO_3^- is reacted with oxygen and produces SO_5^-:

$$SO_3^- + O_2 \rightarrow SO_5^- \quad (12)$$

The following reactions generate SO_4^{2-}:

$$SO_5^- + Mn^{2+}/CS + H^+ \rightarrow Mn^{3+}/CS + HSO_5^- \quad (13)$$

$$HSO_5^- + Mn^{2+}/CS \rightarrow Mn^{3+}/CS + SO_4^- + OH^- \quad (14)$$

$$SO_4^- + Mn^{2+}/CS \rightarrow Mn^{3+}/CS + SO_4^{2-} \quad (15)$$

Design of experiments using Box-Behnken

In this study, the aim at the optimization was to find conditions that gave the maximum oxidation yield. Box-Behnken a design was also identified the relationship between the controllable input parameters and the response variable. Initial concentration of SO_2 in solution after blowing gas is constant in all experiments. Three variables, including temperature (X_1), time (X_2), and nanocatalyst concentration (X_3) are responsible to change the solution conductivity. A three factor, three levels in a Box-Behnken design was established for further optimization for each variable; three levels were promised and encoded by (−1, 0, +1).

The Box-Behnken is a high-quality design in the sense that it could be fitted in the quadratic model. In the current experiments, the effects of three independent variables on response performance and optimal conditions were investigated by engaging with BBD and RSM [23, 24]. Among all RSM designs, Box-Behnken design requires fewer runs (for example 15 runs at three-parameter experimental design) and lets calculations of the response function at intermediate levels and provides estimation of the method efficiency at any experimental point within the range studied through

careful analysis [25]. In this study, the optimization of experimental conditions for SO_2 oxidation using conductivity meter process was studied using Box-Behnken method of RSM. In order to calculate the influence of operating parameters on the SO_2 oxidation, three main factors and three levels for each one was chosen: temperature (°C) (X_1), Reaction time (min) (X_2), and nanocatalyst concentration (g/L) (X_3) as shown in Table 3. Each variable was studied at three levels the low (−1), medium (0) and high (+1). With statistical analysis of the obtained experimental data, a second-order polynomial Eq. (16) was achieved as an empirical model that describes the response surface. The behavior of the system is clarified by the following quadratic equation [26]:

$$Y = \beta_0 + \sum \beta_i X_i + \sum \beta_{ii} X_i^2 + \sum \beta_{ij} X_i X_j, \quad (16)$$

where Y is the response (SO_2 oxidation efficiency), β_0, β_i, β_{ii} and β_{ij} are coefficients of the intercept, linear, square and interaction effects, respectively. The optimum response and also the process parameters were also determined. Test of F in the ANOVA analysis is used for evaluating model variance in residual variance. The variance is almost identical, this ratio is almost one, which indicates that the probability that each of the factors has a significant effect on the response. The statistical significance of the model and the coefficient was analyzed by means of F-test and P value, respectively [27]. In the present study, the SO_2 oxidation process was investigated to treat with different operating conditions such as temperature (10–30 °C), nanocatalyst amount (1.2–6 g/L), reaction time (20–60 min) using (SBR). The number of experiments (n) needed for the development of BBD is defined as:

$$n = 2k(k-1) + C_0 \quad (17)$$

where K is the number of factors and C_0 is the number of repeated central points. Three factors and three levels (for each factor) of BBD were occupied to optimize and check the effect of operation variables on the responses.

A Box-Behnken design was selected to study the effects of three influencing variables on the response (oxidation efficiency). The reward using of Box-Behnken designs to include the fact that they are all spherical designs and require factors to be run at only three levels. Some of these designs also provide orthogonal blocking and if separate runs, need into blocks the Box-Behnken design, designs are available that let blocks be used in such a way that the approximation of the regression parameters for the factor influences are not affected by the blocks [27]. In all 15 runs the experiments were conducted in triplicate and all results attained from the Box-Behnken design is summarized in Table 4. The observed values and predicted response value with residuals for the runs are shown in Table 4. It shows the experimental results of SO_2 oxidation versus model results. The tip

Table 3 Experimental ranges and levels of independent variables

Variables	Range and levels		
	Level 1 (− 1)	Level 2 (0)	Level 3 (+ 1)
Temperature (k), (X_1)	283	298	313
Time (min), (X_2)	20	40	60
Amount of catalyst (g/L), (X_3)	1.2	3.6	6

Table 4 Coded factor levels for a Box-Behnken design of a three-variable system

Observation run	Actual values			SO_2 oxidation efficiency (%)		Residual
	X_1	X_2	X_3	$Y_{experimental}$	$Y_{predicted}$	
1	10	20	3.6	53.000	52.957	0.043
2	30	20	3.6	51.350	51.229	0.121
3	10	60	3.6	53.280	53.314	− 0.034
4	30	60	3.6	51.280	51.587	− 0.307
5	10	40	1.2	38.660	38.741	− 0.081
6	30	40	1.2	39.000	37.014	− 0.014
7	10	40	6	97.800	97.806	− 0.006
8	30	40	6	96.200	96.079	0.121
9	20	20	1.2	38.480	38.559	− 0.079
10	20	60	1.2	37.370	37.196	0.174
11	20	20	6	95.720	95.904	− 0.184
12	20	60	6	98.050	97.981	0.069
13	20	40	3.6	52.540	52.272	0.268
14	20	40	3.6	52.170	52.272	− 0.102
15	20	40	3.6	52.281	52.272	0.009

collections of the diagonal line demonstrate that the difference between the experimental and predicted values was less and good fit of the model is obtained.

All 15 runs were first carried out and used to build a mathematical model to describe the process and the experimental results along with the design matrix are presented in Table 4. It was found that the relationship between SO_2 oxidation yields and the three operating parameters (i.e., temperature, Amount of catalyst and Time) was fitted to a second order polynomial equation. The predicted values of the efficiency were obtained from quadratic model fitting techniques for the Oxidation efficiency (%) using the software minitab 17. The response functions (with the determined coefficients) for Oxidation efficiency are presented by Eq. (18). The ANOVA analysis indicates a linear relationship between the main effects of the amount of nanocatalyst, temperature and time. The final mathematical equation in terms of the actual variable (confidence surface above 95%) as determined by Minitab software 17 is given below:

$$Y = 45.984 - 0.08637x_1 - 0.05556x_2 - 7.33x_3 + 2.6282x_3^2 + 0.01792x_2 \times x_3 \quad (18)$$

The equation reveals that there was a significant synergistic effect (p value = 0.0001) of the concentration of amount of nanocatalyst on the percent SO_2 oxidation efficiency. The amount of nanocatalyst, that had a more coefficient ($7.33x_3$), is more important.

Effect of the variables

To study the effect of three independent variables (x_1, x_2 and x_3) on the characteristics of SO_2 oxidation and entrapment efficiency, analysis of the variance (ANOVA) was performed. The final equations were simplified to contain only significant parameters (p value < 0.05). Suitability of the model was tested using analysis of variance (Table 5). The adjusted R^2 calculates the amount of variation explained by the form after adjusting to the number of parameters in it. The high value of R^2-adjusted designates the high fitness of the model [28]. The ANOVA was also conducted for each answer and the results are presented in Table 5, demonstrating the fact that the predictability of the model is at 95% of confidence surface. Response functions predictions are consistent with experimental data ($R^2 = 99.95$).

Accuracy of the model

The analysis of variance tests is a usual statistical method of the different fields. The analysis of variance provides a statistical process that determines the means of several groups are equal or not. F value is used to test the significance of the model, individual variables and their interactions [29, 30]. The p value is used to check the significance of the coefficient and p value < 0.05 shows that the model is significant and higher than 5% model is not significant. The results were analyzed using the analysis of variance a regression model, the coefficient of determination (R^2), adjusted R-square, statistical-diagnostic and response plots. The F value (48586.56) indirectly suggests that the model is significant. In addition, the p value of the model is less than 0.05, that it is a significant and eligible model. The large value of F indicates that most of the variation in the response can be demonstrated by the regression equation in the Eq. (18). The analysis of variance in (Table 5), Indicates that the second-order polynomial model in term Eq. (18) was statistically significant and adequate to represent the actual

Table 5 ANOVA test for response function

Source	SS	DF	MS	F value	p value	Remarks
Model	7842.11	5	1568.42	48586.56	0.0001	Significant
Linear	6883.57	3	2327.86	72112.38	0.0001	Significant
X_1	5.97	1	5.97	184.89	0.0001	Significant
X_2	0.26	1	0.26	7.92	0.02	Significant
X_3	6977.35	1	6977.35	216144.34	0.0001	Significant
Square	855.58	1	855.58	26,504.02	0.0001	Significant
x_3^2	855.58	1	855.58	26,504.02	0.0001	Significant
2-Way interaction	2.96	1	2.96	91.65	0.0001	Significant
$X_2 \times X_3$	2.96	1	2.96	91.65	0.0001	Significant
Error	0.29	9	0.03			
Lack-of-fit	0.22	7	0.03	0.8	0.632	
Pure error	0.07	2	0.04			
Total	7842.4	14				

$R^2 = 0.9995$ adjusted $R^2 = 0.9997$ predict $R^2 = 0.9992$

relationship between the efficiency and the significant variables, with a very small p value (0.0001) and ($R^2 = 0.9995$). The positive coefficient of the term, X1, indicates that the amount of catalyst is pertaining to a synergy influences on the oxidation efficiency (p value < 0.0001). The ANOVA results also revealed the synergy effect of the amount of catalyst on the oxidation efficiency (p value < 0.0001).

Diagnostics of model adequacy

The natural probability graph is a graphical material that Fig. 10a shows that the remainder of the response is normally distributed. As is evident in Fig. 10a, the obtained point consistently appears on a linear relationship and has indicated that the random error was independently and normally distributed. The results demonstrated that the model applied to the data was significant and sufficient to represent the relationship between the response and the independent variables. Summary of the ANOVA results is shown in (Table). Histogram of Fig. 10b and fitted to value Fig. 10c shows the classification of data's is normal.

The residuals were analyzed to determine the accuracy of the model. To recognize the validity of the prediction, the predicted values of was compared with experimental ones and they are presented in Fig. 11. These results show that the predicted and experimental values are in a good agreement as painted by all points arranged to the diagonal line. The coefficient of the regression model (R^2) was 0.9995, which indicated that the regression model was statistically significant. Moreover, the R^2-Adj value was 99.97%, indicating a high degree of correlation between the experimental and predicted efficiencies.

According to the results, the model in Eq. (17) shows that time has no significant effect on the oxidation of SO_2. These observations are not surprising and, in fact, match the results one at a time [31].

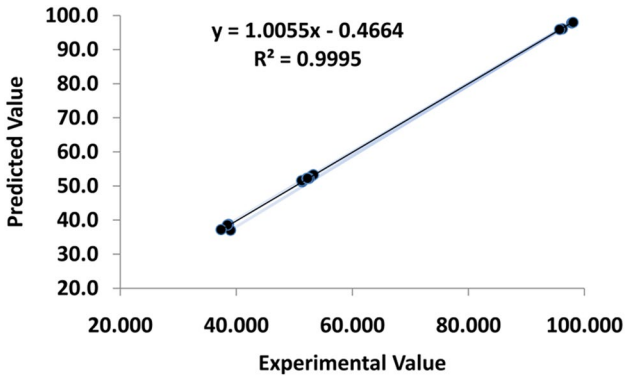

Fig. 11 Actual and predicted plots using Box-Behnken design

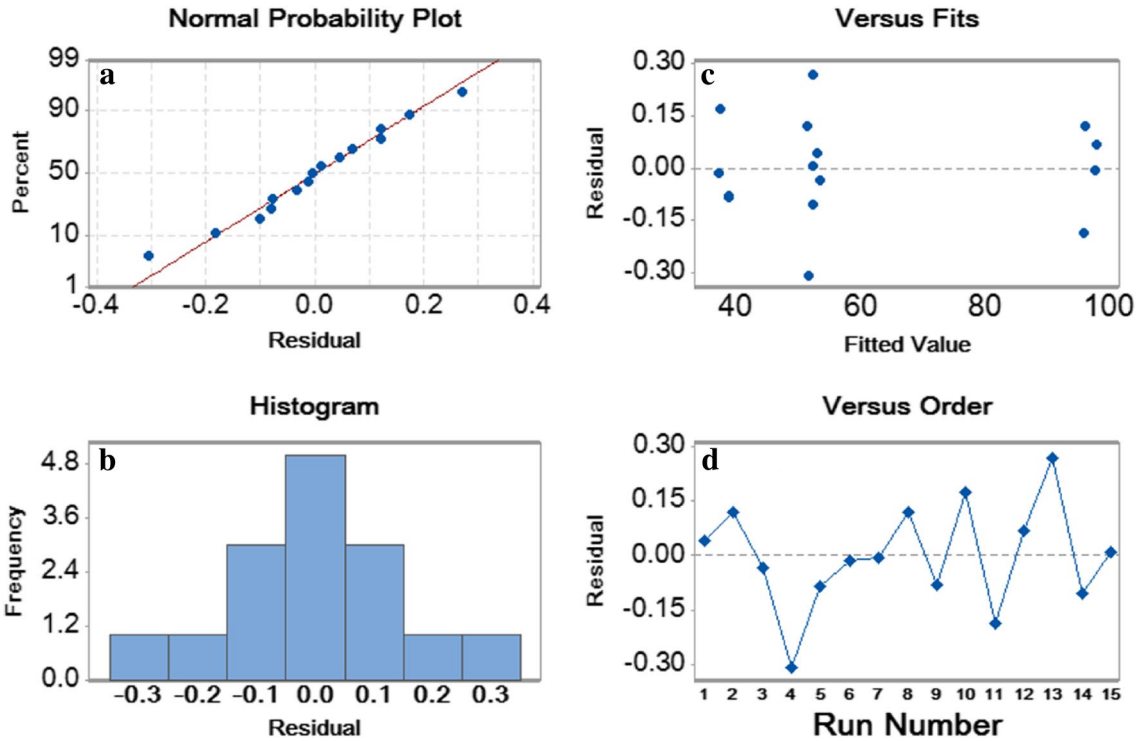

Fig. 10 Diagnostic plots for the Box-Behnken model adequacy. **a** normal probability plot of residuals, **b** Histogram, **c** residual versus fitted values and **d** Residual versus run the numbers

Three-dimensional response surfaces and contour plots

Response surface plots and contour plots and are useful for the model equation and recognizing the character of response surface. A simple examination of the effect of experimental variables on responses is 3D response levels and corresponding contrast components [32]. The resulted surface response 3D plots of efficiency as a function of two independent variables are shown in Fig. 12. Figure 12a, b depicts the interaction of each two variable by keeping the other at its central level for SO_2 oxidation, thus Eq. (18) is used to be drawing the plots. The common interaction between temperature and nanocatalyst amount on the SO_2 oxidation efficiency can be best translated from the response surface contour diagram (Fig. 11a), which indicates that SO_2 oxidation efficiency directly related to nanocatalyst amount.

As shown in Fig. 12a, b efficiency increases with increase in nanocatalyst amount and the temperature (or time) increase is not significant role in increasing the efficiency of SO_2 oxidation. As shown in 3D wafer plot Fig. 12c, efficiency increases with increasing reaction time and the amount of nanocatalyst.

The interaction effects of catalyst concentration and reaction time

The BBD was effectively used to optimize and study the interactive effect of SO_2 oxidation in surface Mn/CS. The contour plot of the influence of the operating parameters on the SO_2 oxidation efficiency is depicted in Fig. 13. Contour plots efficiency (%) versus amount of nanocatalyst and contour plot efficiency (%) versus temperature are presented in Fig. 13a, b. It is important to note that Fig. 13a represents the evolution of influence amount of nanocatalyst versus time. It can be seen that with the increase in amount of nanocatalyst, the efficiency (%) increases.

Under optimal conditions, by means of a catalyst, repeatabilty was perefectly done. Copper Slag has relatively high activity compared to other catalysts such as Mn-activated carbon and Mn/zeolite [4, 6]. This observation is probably related to the higher diffusivity of the reaction intermediates (most of them electrically charged) in a structure. Moreover, the copper slag has the advantage of allowing loading (by ion exchange) more amount of Mn^{2+}.

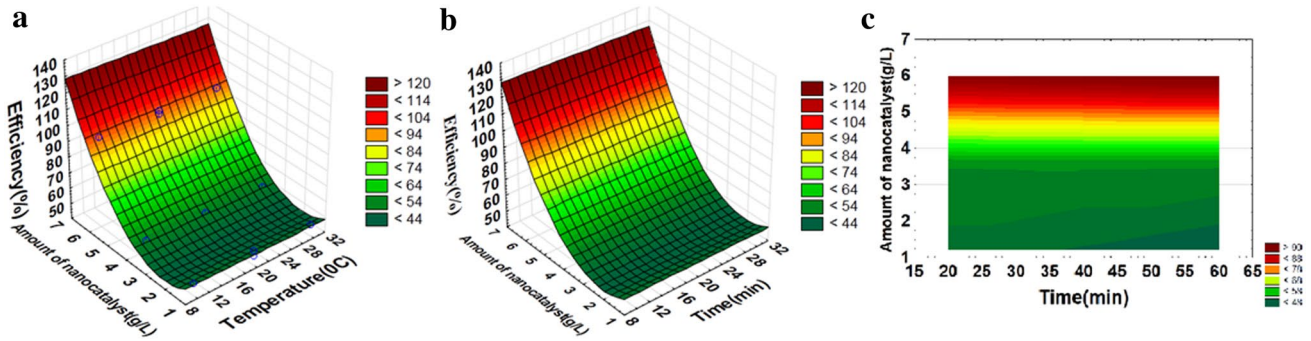

Fig. 12 Response surface plots for the Box-Behnken design: **a** 3D plot of efficiency versus amount of nanocatalyst and temperature, **b** 3D plot of efficiency versus amount of nanocatalyst and time, **c**. 3D wafer plot of amount of nanocatalyst and time

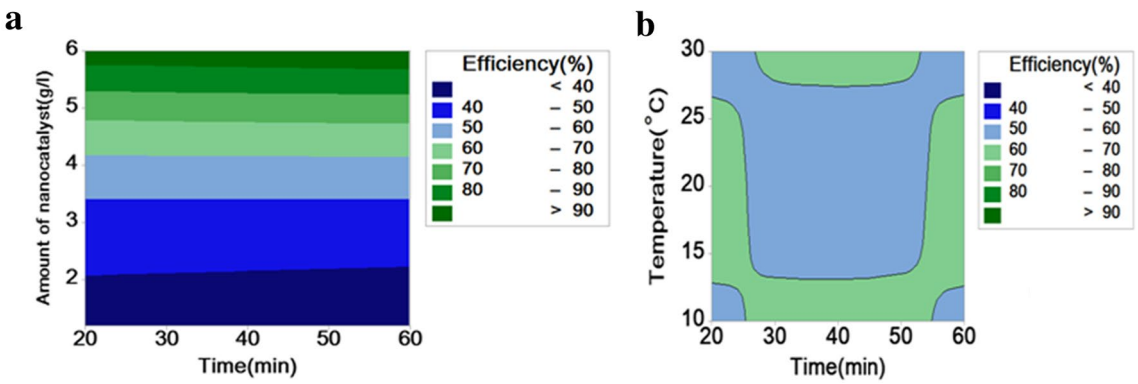

Fig. 13 Contour plot describing for SO_2 oxidation efficiency as a function of amount of nanocatalyst versus temperature. **a** Contour plot of efficiency (%) versus amount of nanocatalyst [g: time (min)]. **b** Contour plot of efficiency (%) versus temperature (°C); time (min)

Conclusions

In this research, oxidation of SO_2 was done using Mn/CS as nanocatalyst in a (SBR) in the low temperature range of 10–30 °C. In order to simulate SO_2 gas industrial in bench scale experimental SO_2 oxidation reaction to oxygen dissolved in aqueous solution catalyzed by Mn/CS was studied using conductivity measurement methods. FESEM images, EDX analysis, FTIR spectroscopy, XRD pattern, XRF, TG/DTA analysis and BET surface area were used to study Mn/CS. High capacity of copper slag for adsorption of manganese ions increases the reaction rate of the oxidation of SO_2 gas. The Box-Behnken design was used to investigate the effect of reaction time, temperature and amount of nanocatalyst on SO_2 oxidation experiments. The SO_2 oxidation process was optimized with respect to three main parameters; temperature, time, and nanocatalyst amount, using BBD. A second polynomial quadratic was fitted with experimental values ($R^2 = 0.9995$).

According to the results, it can be concluded that the application of this SO_2 oxidation process has great potential to be economically and industrially. The fitted model is in a good agreement with the experimental data, so a good correlation coefficient for the quadratic model was gained as 0.9995. The statistical design method predicts a maximum conversion to 99% for the optimum values of three process variables, reaction temperature 10 °C, nanocatalyst amount 6 g/l and reaction time 60 min. The results indicate that for oxidation of SO_2 in the low temperature (10–30 °C) Mn/CS is very active. One of the advantages of this method is the production of sulfuric acid and the removal of SO_2 gas from industrial exhaust. This finding indicates that SO_2 oxidation using Mn/CS is likely related to the excellent catalytic activity of Mn/CS at low temperatures. Maximum efficiency for oxidation of SO_2 at temperature = 283 K, Mn/CS amount = 6 g/L and Time = 60 min was determined.

Catalytic processes have been reported for the oxidation of SO_2 using a hematite catalyst in the presence of hydrogen peroxide as an oxidizer [33]. The use of hydrogen peroxide increases process costs. Another catalyst such as Ce promoted V_2O_5 and CuO/Al_2O_3 are reported for oxidation of sulfur dioxide, which is carried out at high temperatures. In this study, catalytic oxidation is carried out using a new catalyst (Mn/CS) without the use of expensive oxidizers and at ambient temperatures [34, 35].

Acknowledgements The authors wish to thank the Islamic Azad University of Arak, Iran, for financial support.

References

1. Jing W, Guo Q, Hou Y, Ma G, Han X, Huang Z (2014) Catalytic role of vanadium(V) sulfate on activated carbon for SO2 oxidation and NH3-SCR of NO at low temperatures. Catal Commun 56:23–26
2. Hao R, Wang X, Zhao X, Xu M, Zhao Y, Mao X, Yuan B, Zhang Y, Gao K (2018) A novel integrated method of vapor oxidation with dual absorption for simultaneous removal of SO2 and NO: feasibility and prospect. Chem Eng J 333:583–593
3. Sun Y, Zwolinska E, Chmielewski AG (2015) Abatement technologies for high concentration of NO_x and SO_2 removal from exhaust gases: a review. Crit Rev Environ Sci Technol 46(2):119–142
4. Qu YF, Guo JX, Chu YH, Sun MC, Yin HQ (2013) The influence of Mn species on the SO2 removal of Mn-based activated carbon catalysts. Appl Surf Sci 282:425–431
5. Harris E, Sinha B, Pinxteren DV, Tilgner A, Fomba KW, Schneider J, Roth A, Gnauk T, Fahlbusch B, Mertes S, Lee T, Collett J, Foley S, Borrmann S, Hoppe P, Herrmann H (2013) Enhanced role of transition metal ion catalysis during in-cloud oxidation of SO_2. Science 340:727–730
6. Liu Y, Deng J, Xie S, Wang Z, Dai H (2016) Catalytic removal of volatile organic compounds using ordered porous transition metal oxide and supported noble metal catalysts. Chin J Catal 37:1193–1205
7. Mirhosseini SR, Fadaee M, Tabatabaei T, Fadaee MJ (2017) Mechanical properties of concrete with Sarcheshmeh mineral complex copper slag as a part of cementitious materials. Constr Build Mater 134:44–49
8. Zeynolabedin R, Mahanpoor K (2017) Preparation and characterization of nano-spherical CoFe2O4 supported on copper slag as a catalyst for photocatalytic degradation of 2-nitrophenol in water. J Nanostruct Chem 7:67–74
9. Niasar HS, Li H, Das S, Kasanneni TVR, Ray MB, Xu CC (2018) Preparation of activated petroleum coke for removal of naphthenic acids model compounds: Box-Behnken design optimization of KOH activation process. J Environ Manag 211:63–72
10. Thirugnanasambandham K, Sivakumar V, Maran JP (2014) Efficiency of electrocoagulation method to treat chicken processing industry wastewater-modeling and optimization. J Taiwan Inst Chem Eng 45(5):2427–2435
11. Karichappan T, Venkatachalam S, Jeganathan PM, Sengodan K (2013) Treatment of rice mill wastewater using continuous electrocoagulation technique: optimization and modelling. J Korean Chem Soc 57(6):761–768
12. Zhang H, Ran X, Wu X, Zhang D (2011) Evaluation of electro-oxidation of biologically treated landfill leachate using response surface methodology. J Hazard Mater 188(1–3):261–268
13. Kabuk HA, Ilhan F, Avsar Y, Kurt U, Apaydin O, Gonullu MT (2014) Investigation of leachate treatment with electrocoagulation and optimization by response surface methodology. Clean-Soil Air Water 42(5):571–577
14. Metcalfe D, Rockey C, Jefferson B, Judd S, Jarvis P (2015) Removal of disinfection by-product precursors by coagulation and an innovative suspended ion exchange process. Water Res 87:20–28
15. Pavel CC, Popa K (2014) Investigations on the ion exchange process of Cs + and Sr2 + cations by ETS materials. Chem Eng J 245:288–294
16. Shi J, Yao L, Hu C (2015) Effect of CO2 on the structural variation of Na2OWO4/Mn/SiO2 catalyst for oxidative coupling of methane to ethylene. J Energy Chem 24(4):394–400
17. Khorsand Zak A, Abd Majid WH, Ebrahimizadeh Abrishami M, Yousefi R, Parvizi R (2012) Synthesis, magnetic properties and X-ray analysis of Zn0.97X0.03O nanoparticles (X = Mn, Ni, and

Co) using Scherrer and size–strain plot methods. Solid State Sci 14(4):488–494
18. Monshi A, Foroughi MR, Monshi MR (2012) Modified Scherrer equation to estimate more accurately nano-crystallite size using XRD. World J Nano Sci Eng 2:154–160
19. Hargreaves JSJ (2016) Some considerations related to the use of the Scherrer equation in powder X-ray diffraction as applied to heterogeneous catalysts. Catal Struct React 2(1):33–37
20. Mihailova DIM (2010) Characterization of fayalite from copper slags. J Univ Chem Technol Metall 45(3):9
21. Simon G, Vicky K, Peter H (2016) Principals of thermal analysis and calorimetry. The Royal Society Chemistry, London
22. Lan T, Lei L, Yang B, Zhang X, Li Z (2013) Kinetics of the iron(II)- and manganese(II)-catalyzed oxidation of S(IV) in seawater with acetic buffer: a study of seawater desulfurization process. Ind Eng Chem Res 52:4740–4746
23. Rosid SJM, Bakar WAWA, Ali R (2018) Characterization and modelling, optimization on methanation activity using Box-Behnken design through cerium doped catalysts. J Clean Prod 170:278–287
24. Mohadesi M, Shokri A (2017) Evaluation of Fenton and photo-Fenton processes for the removal of p-chloronitrobenzene in aqueous environment using Box-Behnken design method. Desal Wat Treat 81(1):199–208
25. Moradi M, Towfighi Daryan J, Mohamadalizadeh A (2013) Response surface modeling of H2S conversion by catalytic oxidation reaction over catalysts based on SiC nanoparticles using Box-Behnken experimental design. Fuel Process Technol 109:163–171
26. Nam SN, Cho H, Han J, Her N, Yoon J (2018) Photocatalytic degradation of acesulfame K: optimization using the Box-Behnken design (BBD). Process Saf Environ 113:10–21
27. Bagheban Shahri F, Niazi A (2015) Synthesis of modified maghemite nanoparticles and its application for removal of Acridine Orange from aqueous solutions by using Box-Behnken design. J Magn Magn Mater 396:318–326
28. Nur W, Wan A, Azelee W et al (2014) Deep desulfurization of model diesel by extraction with N, N -dimethylformamide: optimization by Box-Behnken design. J Taiwan Inst Chem Eng 45(4):1542–1548
29. Shen C, chang Y, Fang L, Min M, Xiong H (2016) Selective removal of copper with polystyrene–1,3-diaminourea chelating resin: synthesis and adsorption studies. New J Chem 40(4):3588–3596
30. Saghi M, Mahanpoor K (2017) Photocatalytic degradation of tetracycline aqueous solutions by nanospherical α-Fe2O3 supported on 12-tungstosilicic acid as catalyst: using full factorial experimental design. Int J Ind Chem 8:297–313
31. Li Y, Zhou S, Fang L, Li J, Zheng X, Jiang J, Xiong C (2016) Adsorptive removal of Ni(II) from aqueous solution on 110-H resin: optimization through response surface methodology. Desalin Water Treat. 57(23):10710–10722
32. Ravanfar R, Tamaddon AM, Niakousari M, Moein MR (2016) Preservation of anthocyanins in solid lipid nanoparticles: optimization of a microemulsion dilution method using the Placket-Burman and Box- Behnken designs. Food Chem 199:573–580
33. Ding J, Zhong Q, Zhang S, Song F, Bu Y (2014) Simultaneous removal of NOX and SO2 from coal-fired flue gas by catalytic oxidation-removal process with H2O2. Chem Eng J 243:176–182
34. Mazidi M, Mosayebi Behbahani R, Fazeli A (2017) Ce promoted V2O5 catalyst in oxidation of SO2 reaction. Appl Catal B-Environ 209:190–202
35. Kameda T, Kodama A, Yoshioka T (2013) Simultaneous removal of SO2 and NO2 using a Mg–Al oxide slurry treatment. Chemosphere 93:2889–2893